Cloud Impact on Surface Altimetry From a Spaceborne 532-nm Micropulse Photon-Counting Lidar: System Modeling for Cloudy and Clear Atmospheres

Yuekui Yang, Alexander Marshak, Stephen P. Palm, Tamás Várnai, and Warren J. Wiscombe

***Abstract*—This paper establishes a framework that simulates the behavior of a spaceborne 532-nm micropulse photon-counting lidar in cloudy and clear atmospheres in support of the ICESat-2 mission. Adopted by the current mission design, the photon-counting system will be used to obtain surface altimetry for ICESat-2. To investigate how clouds affect surface elevation retrievals, a 3-D Monte Carlo radiative transfer model is used to simulate the photon path distribution and the Poisson distribution is adopted for the number of photon returns. Since the photon-counting system only registers the time of the first arriving photon within the detector "dead time," the retrieved average surface elevation tends to bias toward higher values. This is known as the first photon bias. With the scenarios simulated here, the first photon bias for clear sky is about 6.5 cm. Clouds affect surface altimetry in two ways: 1) Cloud attenuation lowers the average number of arriving photons and hence reduces the first photon bias, and 2) cloud forward scattering increases the photon path length and makes the surface appear further away from the satellite. Compared with that for clear skies, the average surface elevation detected by the photon-counting system for cloudy skies with optical depth of 1.0 is 4.0–6.0 cm lower for the simulations conducted. The effect of surface roughness on the accuracy of elevation retrievals is also discussed.**

***Index Terms*—ICESat-2, lidar altimetry, path delay, polar cloud, radiative transfer.**

I. Introduction

DUE TO THE vast volume of the Antarctic and Greenland ice sheets, a small change of 0.1% in the average ice thickness would result in a global sea level difference of 8.3 cm [1]. Hence, accurate knowledge of ice-sheet mass balance is critical in predicting future sea-level rise and global climate change (e.g., [2] and [3]). Satellite observations provide the only feasible way to monitor the entire ice sheets (e.g., [3]–[7]). To serve this purpose, NASA launched the Ice, Cloud, and land Elevation Satellite (ICESat) in 2003. Onboard ICESat was the Geoscience Laser Altimeter System (GLAS), which was designed to obtain accurate surface elevation on a global scale. One science objective of ICESat was to detect long-term elevation changes with an accuracy of < 1.5 cm/year over ice-sheet areas of 100×100 km^2. Since its launch, ICESat has provided data that contribute significantly to the understanding of the polar ice sheets (e.g., [8]–[10]).

Understanding the change of ice sheets requires a long-term elevation time series. In 2007, the National Research Council's Decadal Survey recommended ICESat-2 as a successor of ICESat and as one of the top priority NASA missions [11]. As stated by the Decadal Survey, "the proposed ICESat-2 measurements directly address the contribution of changing terrestrial ice cover to global sea level. As such, these measurements are key to projecting the impact of sea-level change on growing populations and infrastructure along almost all coastal regions." Compared with that of ICESat, which uses a 1064-nm lidar with analog detection, the significantly improved design of ICESat-2 adopts a 532-nm micropulse photon-counting lidar system with single photon detectability. The system will measure the time of flight of the arriving photons that are reflected by the surface to deduce the elevation of the underlying terrain.

Since every photon emitted by the lidar system will travel through the atmosphere, clouds can certainly affect the flight time of the arriving photons. Forward scattering by cloud particles increases the photon path length, thus resulting in biases in ice-sheet elevation measurements known as atmospheric path delay. Previous studies on this topic have been focused on the effect of clouds on the altimetry from a GLAS-like analog detection system [12]–[14]. To ensure the accuracy of ICESat-2 surface elevation measurements, it is critical to understand how clouds would affect the travel time of arriving photons for the 532-nm photon-counting system. To address this issue, we first establish a framework that simulates the behavior of this system in both cloudy and clear atmospheres, and then, the effect of clouds is studied within this framework.

Manuscript received March 8, 2010; revised February 14, 2011; accepted April 23, 2011. This work was supported by the National Aeronautics and Space Administration's ICESat-2 Science Definition Project.

Y. Yang is with the Universities Space Research Association, Columbia, MD 21044-3432 USA, and also with the NASA Goddard Space Flight Center, Greenbelt, MD 20771 USA (e-mail: Yuekui.Yang@nasa.gov).

A. Marshak and W. J. Wiscombe are with the NASA Goddard Space Flight Center, Greenbelt, MD 20771 USA (e-mail: alexander.marshak@nasa.gov; warren.j.wiscombe@nasa.gov).

S. P. Palm is with the NASA Goddard Space Flight Center, Greenbelt, MD 20771 USA, and also with Science Systems and Applications, Inc., Lanham, MD 20706-6239 USA (e-mail: Stephen.p.palm@nasa.gov).

T. Várnai is with the NASA Goddard Space Flight Center, Greenbelt, MD 20771 USA, and also with the Joint Center for Earth Systems Technology, University of Maryland Baltimore County, Baltimore, MD 21228 USA (e-mail: tamas.varnai@nasa.gov).

Digital Object Identifier 10.1109/TGRS.2011.2153860

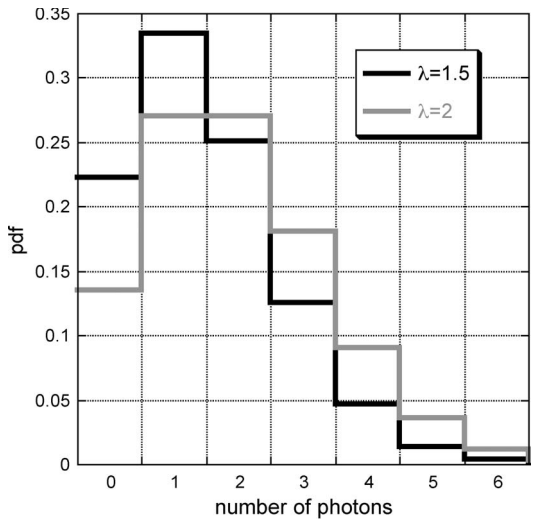

Fig. 1. Photon returns under Poisson distribution assumption. λ is the expected number of photon returns.

The remainder of this paper is organized into six sections. Section II describes the basic approach we used to model the system. In Section III, we discuss the first photon bias of the system under clear-sky condition. Section IV demonstrates how the presence of clouds results in biases in surface elevation retrievals through reducing first photon bias and increasing photon path length. Section V discusses the effects of cloud height and cloud microphysics. In Section VI, the uncertainty of surface elevation retrieval is estimated for both smooth and rough surfaces. The main results are summarized in Section VII.

II. Modeling the Photon-Counting System

The current design of the ICESat-2 lidar system requires the ability to detect a single photon event. After one event is recorded, the system will not respond to the next arriving photon until the detector dead time ($\sim$5 ns) is exceeded. A dead time of 5 ns is equivalent to a space range of 75 cm (for light to travel back and forth). The emitted laser pulsewidth is 1 ns. So essentially, for each pulse over a flat smooth surface, the photon-counting system only records the first arriving photon that is reflected by the surface. The telescope field of view (FOV) corresponds to 40 m in diameter on the surface from a nominal orbit altitude of 600 km.

As a stochastic process, the number of photon returns at the detector under clear-sky condition can be simulated with a Poisson distribution (e.g., [15] and [16])

$$p_k(\lambda) = \lambda^k \exp(-\lambda)/k! \tag{1}$$

where $p_k(\lambda)$ is the probability of having k arriving photons when the expected number is λ.

Fig. 1 shows the photon return distribution for $\lambda = 1.5$ and 2.0. For Poisson distribution, mean = variance = λ [17, p. 111–119]. Hence, the number of received photons at the detector fluctuates about its mean λ with a standard deviation of $\sqrt{\lambda}$. From Fig. 1, the probabilities of having no photon return ($k = 0$) for $\lambda = 1.5$ and 2.0 are 22.3% and 13.5%, respectively. For the ICESat-2 photon-counting system, it is more important to know the probability of having at least one arriving photon. Let $p_{>0}(\lambda)$ be the probability of receiving at least one photon when the average number of photon return is λ. Then, from (1)

$$p_{>0}(\lambda) = 1 - p_0(\lambda) = 1 - \exp(-\lambda) \tag{2}$$

where $p_0(\lambda)$ is the probability of having no photon return.

The current design of the ICESat-2 system requires $p_{>0}(\lambda)$ to be 0.8 for clear air over ice surface. This can be closely approximated by assuming that $\lambda = 1.5$ (for $\lambda = 1.5$, $p_{>0}(\lambda) = 0.78$). Hereafter in this study, unless pointed out explicitly, a Poisson distribution with $\lambda = 1.5$ is utilized to simulate the number of returns for the ICESat-2 photon-counting system.

The previous discussion is for clear sky only. When a cloud is present, it will have two effects on the system. First, part of the photons emitted by the laser will be scattered away by the cloud particles, and hence, less photons will arrive at the detector. We simulate this process with our 3-D Monte Carlo model that has been validated by the International 3-D Radiation Code project [18]. To study this mechanism, we start with a cloud example located at 0.5–1.0 km. Since we focus on clouds over polar ice sheets with cloud optical depth (COD) < 2.0 (so that they could be penetrated by the laser [19]), the cloud particle phase is presumed to be ice. We adopt the phase function used by the Moderate Resolution Imaging Spectroradiometer (MODIS) ice cloud property retrievals, which is derived based on a mixture of particle habits [20]. For this example, the cloud particle effective radius r_e is assumed to be 20 μm. The effect of cloud particle size and shape and cloud height will be discussed in Section V. Note that, in our simulations, aerosols and Rayleigh scattering are not accounted for. Aerosols are generally optically thin over ice sheets, and Rayleigh scattering has been shown to have very limited impact on surface elevation retrievals [14].

Fig. 2(a) shows the results of photon return as a function of COD. As expected, when COD increases, not only the mean number of photons that arrive at the detector decreases but also the number of laser shots that have at least one photon return. For example, for COD $= 0.1$, the average photon return is 1.3 and the laser shots that have at least one photon coming back is 73%; for COD $= 1.0$, the numbers drop to 0.5 and 40%, respectively. Fig. 2(b) compares the distributions of photon returns of clear sky, i.e., COD $= 0.1$ and COD $= 1.0$. As shown in the figure, for thicker clouds, the number of laser shots that have multiple photon returns declines significantly. Interestingly, the number of shots with exactly one photon coming back for COD $= 1.0$ is higher than that for the clear sky and COD $= 0.1$. This is due to the fact that many of the laser shots that would have multiple returns for clear sky or COD $= 0.1$ have only one return left for COD $= 1.0$.

The second effect that clouds have on the photon-counting system is that forward scattering by cloud particles skews the probability distribution of photon arrival time. Assuming that the emitted laser pulse has a Gaussian shape with a pulsewidth of 1 ns, then for clear sky, the probability distribution of the arrival time of the reflected photons would still be Gaussian. However, when clouds are present, scattering by cloud particles

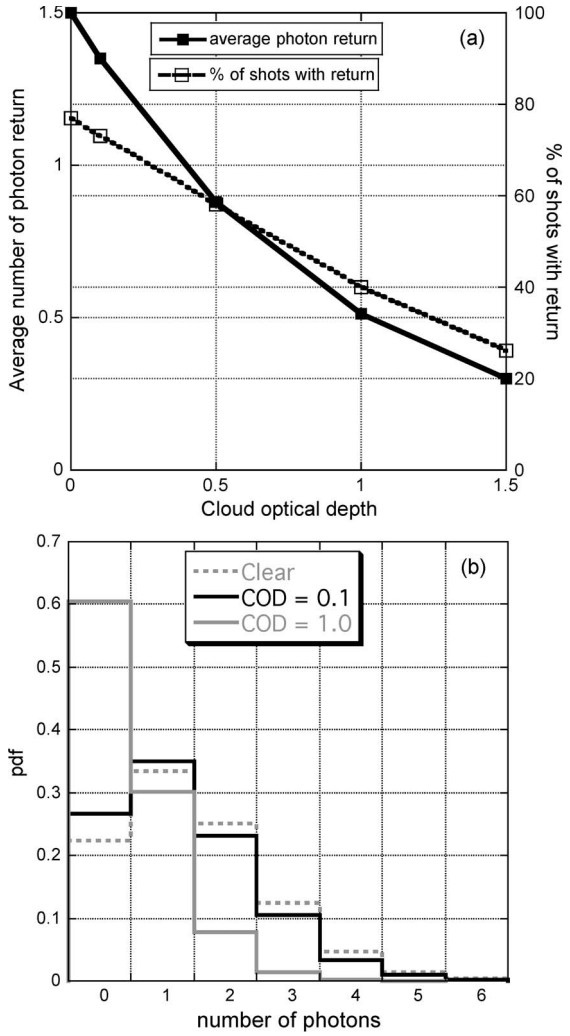

Fig. 2. Cloud impact on photon returns. (a) (Solid line) Average photon returns and (dashed line) percentage of laser shots that have at least one photon return. (b) Distribution of photon returns for (dashed gray line) clear sky and cloudy sky with (solid black line) optical depth of 0.1 and (solid gray line) optical depth of 1.0. Cloud was at 0.5–1.0 km. Telescope FOV $= 40$ m.

increases photon path length, hence creating atmospheric path delay [12], [14]. Fig. 3 shows this point with the photon arrival time (equivalently, photon path length) translated into position relative to the surface. The distribution for cloudy sky is skewed right because of the probability of a photon being delayed by scattering. Same as in Fig. 2, the cloud used in the Fig. 3 simulation is located at 0.5–1.0 km and the MODIS phase function with $r_e = 20$ μm is used. As will be discussed in Section V, the path delay caused by this effect is also a function of cloud height and particle size and shape.

III. First Photon Bias for Clear-Sky Measurements

Since, for each pulse over a flat smooth surface, the photon-counting system only records the time of the first arriving photon that is reflected by the surface, if there are multiple photons arriving at the sensor, the surface elevation results will be biased toward the photon that arrives the earliest, which will make the surface appear closer to the satellite and hence create the first

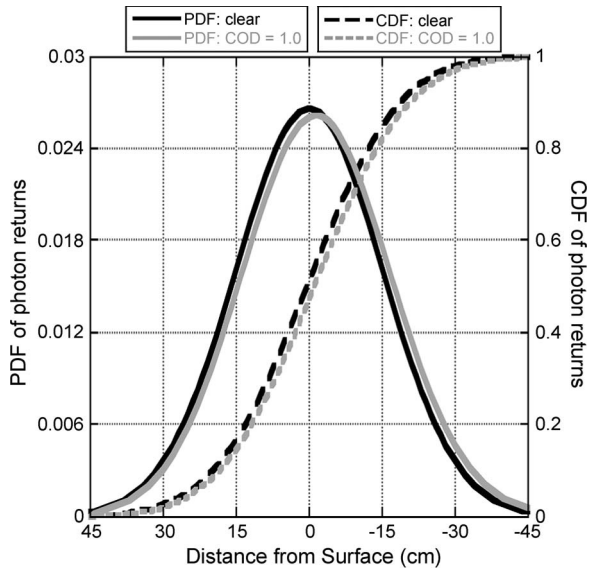

Fig. 3. Cloud impact on photon path length distribution. Solid lines are the probability distribution functions, and dashed lines are the cumulative distribution functions. Plotted are for (black lines) clear sky and (grey line) cloudy sky with COD 1.0. Cloud was at 0.5–1.0 km. MODIS phase function for $r_e = 20$ μm was used. FOV $= 40$ m.

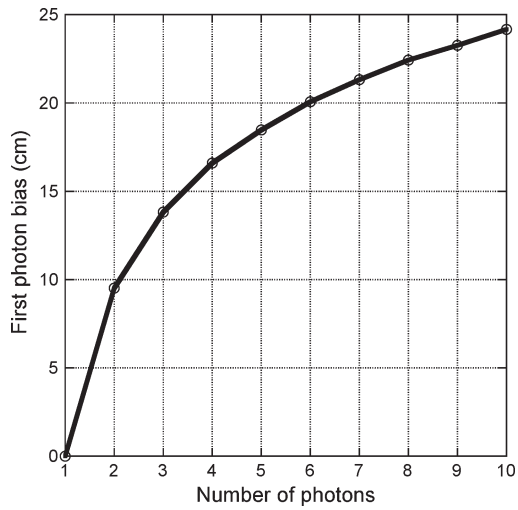

Fig. 4. Monte Carlo-simulated first photon bias as a function of photon returns. Gaussian photon path distribution with standard deviation of 15 cm (1 ns for light to travel back and forth) was used.

photon bias. To simulate the first photon bias of N arriving photons with the Monte Carlo method, N random numbers that represent photon travel time are generated according to the Gaussian distribution that matches the laser pulse (pulsewidth: 1 ns). Since the detector only registers the time of the first photon, the smallest number is recorded. Then, the recorded time is translated into apparent surface elevation based on the speed of light. Fig. 4 shows the results for 10 000 simulated laser shots. True surface elevation is set at zero. As shown in the figure, if there is only one photon return for every laser shot, the first photon bias does not exist. The bias increases with the number of photon arrivals. If there are two arriving photons for every laser pulse, the bias is 9.5 cm. It reaches 18.5 cm if the arriving photon number is 5.

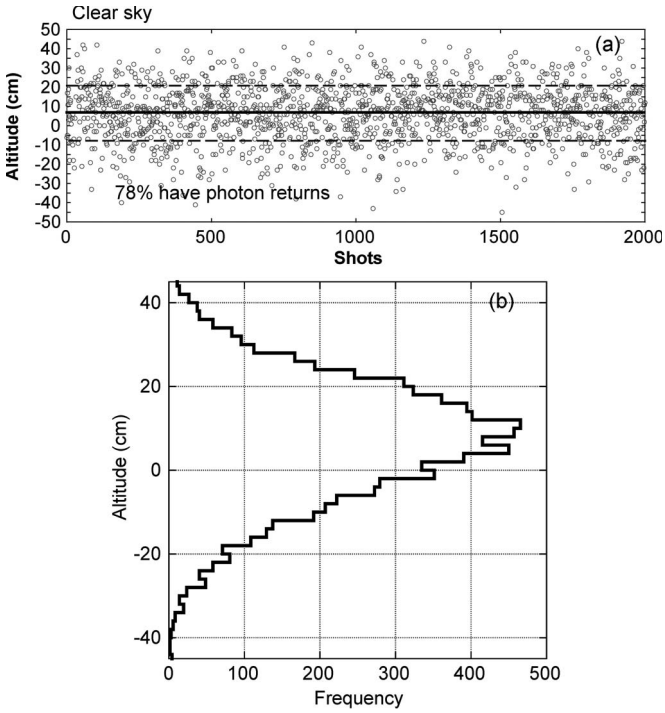

Fig. 5. First photon bias under clear-sky conditions. (a) Elevation retrievals simulated by the Monte Carlo method. Shown in the plot are the first 2000 laser shots out of the 10 000 simulated. The solid line gives the mean surface elevation derived from the arriving photons, and the dashed lines mark the standard deviation. The number of arriving photons for each realization follows the Poisson distribution with $\lambda = 1.5$. (b) Distribution of elevation retrievals for the 10 000 laser shots simulated.

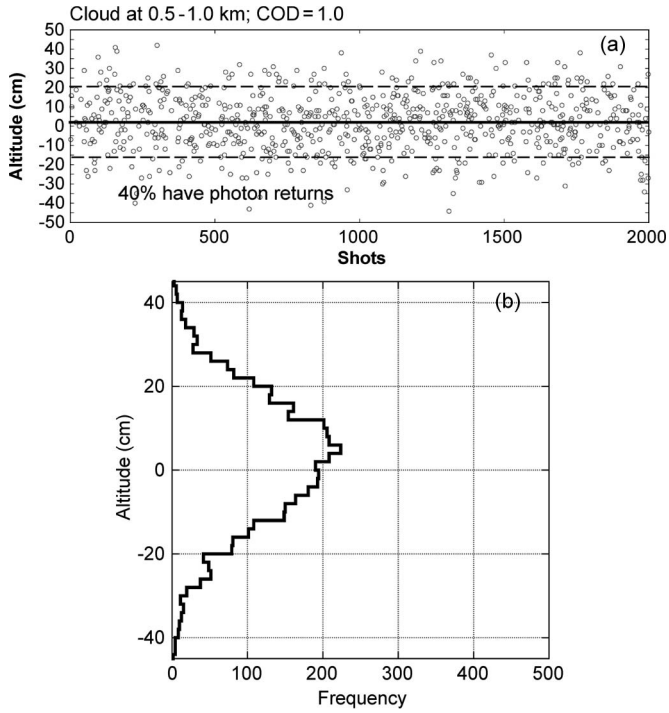

Fig. 6. Cloud impacts on first photon bias. (a) Same as Fig. 5(a) except for cloudy condition with COD $= 1.0$. (b) Same as Fig. 5(b) except for cloudy condition with COD $= 1.0$.

Let us examine the results under realistic clear-sky conditions. Assuming we fire 10 000 laser shots, the number of arriving photons would follow the Poisson distribution with $\lambda = 1.5$. In simulations, the apparent surface elevation can be derived as long as there is at least one photon return. Fig. 5(a) shows the first 2000 shots out of the 10 000 simulated. As determined by the Poisson distribution, 78% of the realizations have at least one photon return. The results show that when averaged over all the 10 000 shots, the mean surface elevation derived from the arriving photons is 6.5 cm higher than the actual surface, which is a direct result of the first photon bias. Fig. 5(b) shows the histogram of surface elevation derived from arriving photons. If the first photon bias did not exist, the histogram would have been Gaussian with mean $= 0$ and standard deviation $= 15$ cm. Due to the first photon bias, the mean of the histogram becomes 6.5 cm and the standard deviation is 14.4 cm.

IV. Cloud Impacts on Elevation Retrievals

As aforementioned, for the photon-counting system, clouds affect surface elevation retrieval in two ways. First, clouds lower the average number of arriving photons. As discussed in Section III, due to the first photon bias, less arriving photons makes the surface appear further from the satellite (at a lower elevation) compared with clear sky. Second, some of photons registered at the detector have gone through scattering by cloud particles. The scattering increases the photon path and also makes the surface appear to be lower. The second mechanism has been investigated rather thoroughly by previous studies [12]–[14]. The combined effect is that clouds make the surface appear lower compared with clear-sky measurements. It is worth noticing that the first photon bias results in surface elevation retrievals higher than the real value, while the effects of clouds work against the first photon bias. Ironically, the surface elevation retrievals under cloudy sky may be closer to the real value than retrievals under clear sky. In practice, there are multiple ways to correct the first photon bias; a common way is to apply the correction based on clear-sky properties. If this is the case, the retrievals under cloudy-sky conditions will be biased.

The simulation of the behavior of the photon-counting system under cloudy sky can be broken into two steps. First, the arriving photon number and photon path distributions for different CODs are simulated with our 3-D radiative transfer model; second, for each laser shot, the arrival time of the first photon is calculated with the same Monte Carlo method as described in Section III except that the random numbers that represent photon travel time are generated according to the simulated photon path distributions instead of a Gaussian distribution.

Similar to Figs. 5(a), Fig. 6(a) shows the first 2000 laser shots out of the 10 000 simulated under cloudy sky with COD $= 1.0$. Compared with the 78% for clear sky, only 40% of the shots have at least one photon return. When averaged over all the 10 000 shots, the mean surface elevation derived from the arriving photons is 1.8 cm higher than the real value (0 cm). For clear sky, due to first photon bias, the derived surface elevation is 6.5 cm; hence, if we use the mean surface elevation derived from each pulse as the final retrieval, the surface elevation retrieved for COD $= 1.0$ is much closer to the real surface than that for clear sky. Fig. 6(b) shows the histogram of surface

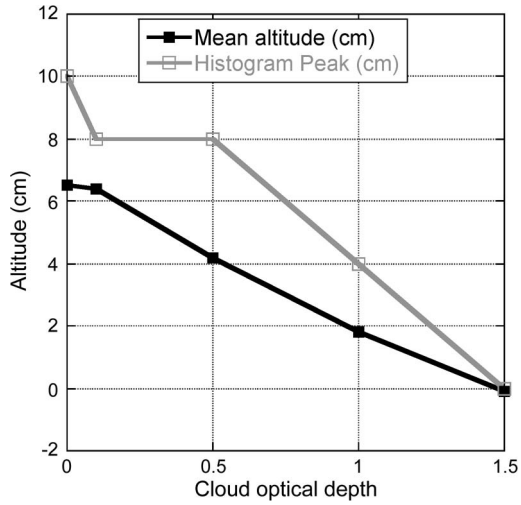

Fig. 7. Cloud impacts on retrieved surface elevation. The black line is the mean elevation, and the gray line is the elevation where the histogram mode is located.

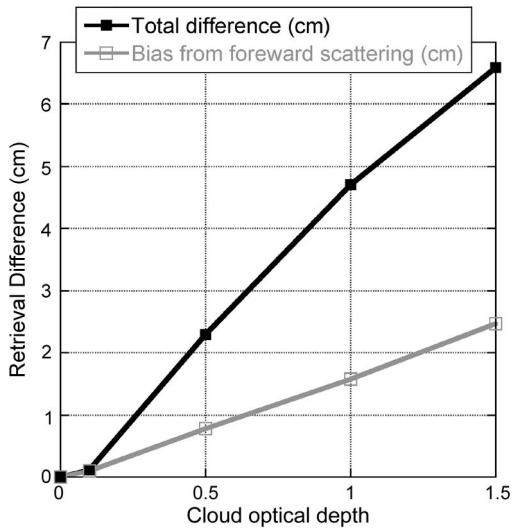

Fig. 8. (Black line) Total difference between surface elevation retrievals under clear- and cloudy-sky conditions and (gray line) the part that is resulted from cloud forward scattering alone.

elevation derived from the registered arriving photons. The histogram peaks at 4.0 cm with a mean of 1.8 cm and a standard deviation of 18.0 cm. As can be seen, clouds lower the retrieved surface elevation compared with clear sky but increase the standard deviation of the histogram.

In addition to using the mean of surface elevations derived from each individual pulse as the final retrieval, we can also use the mode of the histogram. Fig. 7 compares the impact of clouds on surface elevation retrieval for both methods. As expected, as COD increases, both the mean and the mode of the histogram decrease. From the figure, generally, the histogram mode gives higher elevation than the mean. It is interesting that for COD $= 1.5$, the retrievals of both methods essentially give the true surface elevation for the simulations conducted here. As demonstrated earlier, this results from the fact that the presence of clouds mitigated the first photon bias under clear sky.

As aforementioned, if the correction of first photon bias will be based on clear-sky results, the difference between the retrievals under clear- and cloudy-sky conditions is the bias caused by clouds, which consists of two parts: the part that is created by the clouds' lowering the average number of arriving photons and the part that is caused by the path delay due to cloud forward scattering. Fig. 8 shows the total bias and the part that is induced from cloud forward scattering; the difference of these two curves is the part that is caused by the clouds' lowering the number of arriving photons. Obviously, the bias increases with COD. At COD $= 1.0$, the total bias is 6.5 cm $-$ 1.8 cm $= 4.7$ cm, to which forward scattering contributes 1.6 cm (34%).

V. Effects of Cloud Altitude and Particle Microphysics

We have demonstrated the two mechanisms through which a cloud affects surface altimetry from a photon-counting system using a cloud at 0.5–1.0 km with MODIS phase function for $r_e = 20$ μm. However, the biases caused by both mechanisms are a function of cloud altitude and cloud microphysics.

Let us first look at how cloud altitude and cloud microphysics affect the average number of photon returns and, subsequently, the first photon bias. As shown in Fig. 9(a), for the given cloud microphysics and optical depth, the lower the cloud, the higher is the number of photon returns. This is due to the fact that for lower clouds, photons that experienced multiple scattering have a larger chance to stay in the FOV [14]. Similarly, given cloud altitude and optical depth, the more forward scattering, the larger the number of photon returns [Fig. 9(b)]. It is well known that for a given particle shape, the larger the r_e, the more significant the forward peak of the phase function; hence, as shown in Fig. 9(b), when using the MODIS phase functions, clouds with $r_e = 50$ μm have more photon returns than clouds with $r_e = 20$ μm, which, in turn, have more photon returns than clouds with $r_e = 10$ μm. Fig. 9(b) also shows the photon returns for clouds consisting of hollow column and bullet rosette particles with $r_e = 20$ μm. As can be seen in the figure, for the same r_e, the cloud with the hollow column particles have more photon returns compared with the cloud with MODIS phase function, while the cloud with the bullet rosette particles have fewer photon returns. This result can also be explained by the fact that the phase function of the hollow column particles has the largest forward peak among the three, while that of the bullet rosette particles has the smallest. As explained in previous sections, the difference in the number of photon returns between clear and cloudy conditions determines the difference in the first photon bias. Clouds resulting in fewer photon returns lead to larger differences in surface elevation retrievals when compared with clear sky.

Following the procedure described in Section IV, we calculate the effect of cloud altitude and particle microphysics on the differences in surface elevation retrievals between clear- and cloudy-sky conditions. The results are shown in Fig. 10. Fig. 10(a) and (b) shows the effect of cloud altitude. As shown in Fig. 10(b), the lower the cloud, the larger the difference caused by cloud forward scattering. This is consistent with previous studies [12], [14]. On the other hand, the

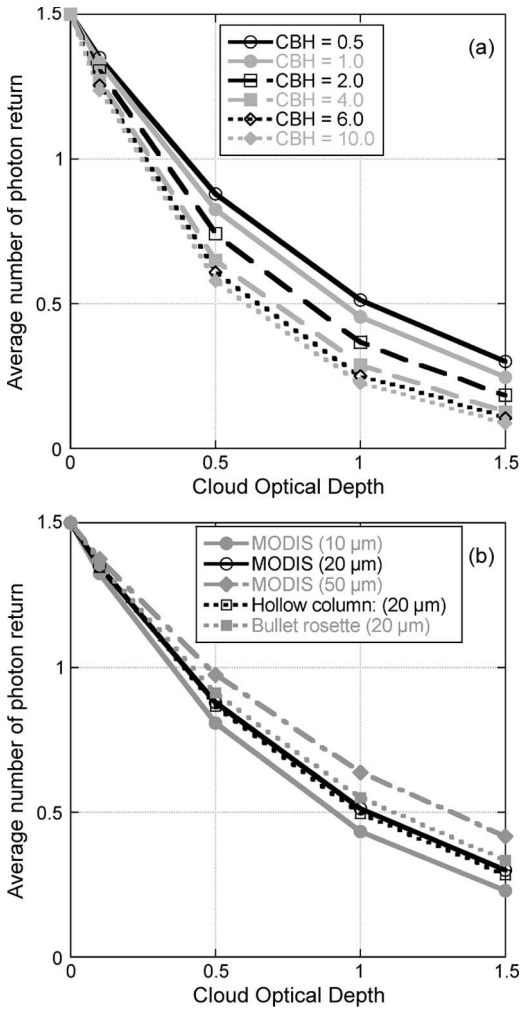

Fig. 9. Effect of cloud altitude and cloud particle size and shape on the number of photon return. (a) Effect of cloud altitude. MODIS phase function for $r_e = 20$ μm is used, and cloud thickness is assumed to be 0.5 km. (b) Effect of cloud particle size and shape. Clouds are located at 0.5–1.0 km.

lower the cloud, the smaller the contribution of first photon bias differences. For the combinations of the two mechanisms [Fig. 10(a)], the total differences are not a monotonic function of cloud altitude and the value range is small. For example, for COD $= 1.0$, the differences among different cloud altitudes are within 15%. Fig. 10(c) and (d) shows the effect of cloud particle size and shape. Different particle sizes and shapes correspond to different phase functions. As shown in Fig. 9(b), the cloud phase function with a larger forward peak leads to smaller differences in first photon bias between clear and cloudy conditions. Also, for the same COD and cloud altitude, same surface condition, and same atmosphere profile, phase functions with larger forward peaks cause smaller path delays [Fig. 10(d)]. Therefore, the total differences between clear- and cloudy-sky retrievals are smaller for phase functions with larger forward peaks [Fig. 10(c)]. From Fig. 10(a) and (c), compared with clear sky, the average surface elevation detected by the photon-counting system for cloudy sky with optical depth 1.0 is 4.0–6.0 cm lower for the simulations conducted. It should be pointed out, however, that for fixed COD, even though the cloud particle size has a significant impact on surface altimetry, the impact of the particle shape is relatively small. For example [Fig. 10(c)], for COD $= 1.0$, the differences among MODIS, bullet rosette, and hollow column particles are within 15%.

VI. Altimetry Uncertainties and Surface Roughness

In practice, since only the time of the first arriving photon reflected by the surface is registered at the detector, there is essentially no way to tell whether the photon comes from a cloud or the surface or just from the noise. Hence, for a photon-counting system, it is not practical to derive a surface elevation for each laser shot. Statistics provided by many shots is needed in order to retrieve the surface elevation. Our discussion so far has focused on understanding the general behavior of the photon-counting system, which is why we based our analysis on the statistics of 10 000 laser shots. The spacing of the ICESat-2 footprint is currently set at 70 cm. It has been proposed that surface elevation retrieval should be done based on the statistics of 100 shots. If one value is obtained for every 100 shots (70 m), then over the course of 10 000 shots (7 km), 100 values can be retrieved. Fig. 11 shows the results for a flat surface. The error bars are the standard error of the derived values within each 100 shot packet. They provide the uncertainty of the retrievals. For clear sky [Fig. 11(a)], the uncertainty is 1.6 cm on average. To demonstrate the effect of clouds, again, we use a cloud located at 0.5–1.0 km with the MODIS phase function for $r_e = 20$ μm. For COD $= 1.0$ [Fig. 11(b)], the uncertainty in surface elevation retrieval increases to 2.5 cm.

Elevation retrievals are also affected by surface roughness. More advanced methods have been used in surface roughness studies (e.g., [21]–[25]). Here, we adopt a much simpler approach, using the standard deviation of small-scale elevation fluctuations from the linear trend over a certain distance as the definition of surface roughness (e.g., [26] and [27]). The ice sheet surface roughness varies considerably by region. Using airborne laser altimetry data, a recent study by van der Veen *et al.* [26] showed that the surface roughness of the northern half of the Greenland Ice Sheet is 8 cm or less. Through analysis of ICESat data, another study by Yi *et al.* [27] found that the roughness of central Greenland is around 10 cm and the roughness increases toward the coastal areas, where it can reach the meter level. We simulate surface roughness as random elevation change that follows the Gaussian distribution. Fig. 12(a) shows the uncertainty of surface elevation retrievals from 100 laser shots as a function of surface roughness. As shown in Fig. 12(a), if a surface roughness of 10 cm is added, uncertainty of surface elevation retrievals based on 100 laser shots is around 2.0 cm for clear sky and 3.0 cm for COD $= 1.0$ on average. Compared with flat surface, the uncertainty increased by 25% and 20% for clear sky and for COD $= 1.0$, respectively. As the surface roughness increases, the differences between clear- and cloudy-sky surface elevation retrievals increase as well.

Uncertainty can be lowered through averaging over larger distance. For example, if the uncertainty of one individual retrieval is u, then after averaging over N retrievals, the uncertainty would be lowered to $u/\sqrt{N}$. An important question is as follows: Over what distance do the surface elevation retrievals

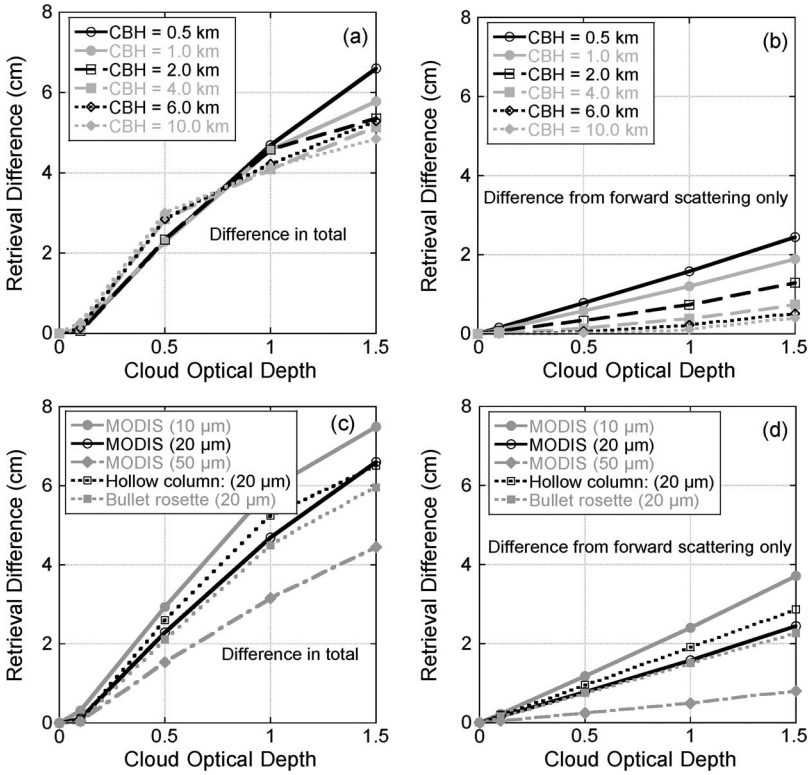

Fig. 10. Differences between surface elevation retrievals under clear- and cloudy-sky conditions. The total difference consists of two parts: The part caused by the clouds' lowering the average number of arriving photons and the part caused by the path delay due to cloud forward scattering. (a) Total difference for different cloud altitude. (b) Part of the difference resulted from cloud forward scattering alone for clouds corresponding to (a). (c) Same as (a) but for different cloud particle size and shape. (d) Same as (b) but for clouds corresponding to (c).

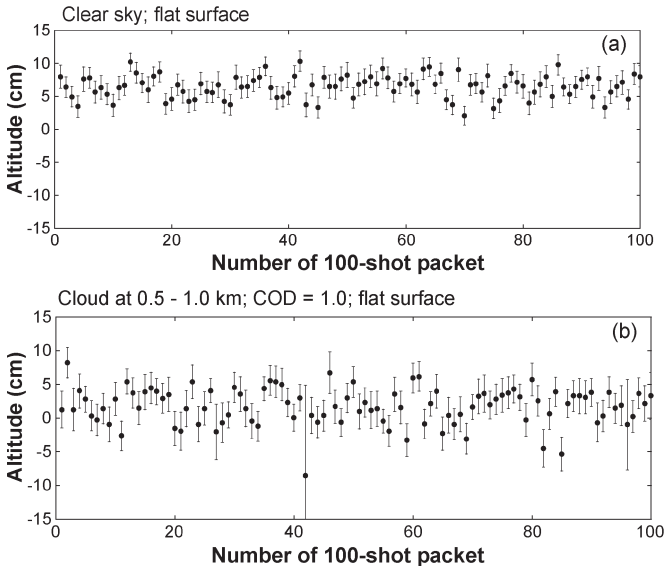

Fig. 11. (Black dots) Surface elevation retrievals using 100-shot packet and the standard error within the 100 shots for (a) clear sky and (b) COD $= 1.0$. Cloud is located at 0.5–1.0 km, and the MODIS phase function with $r_e = 20$ μm was used. Surface is assumed flat.

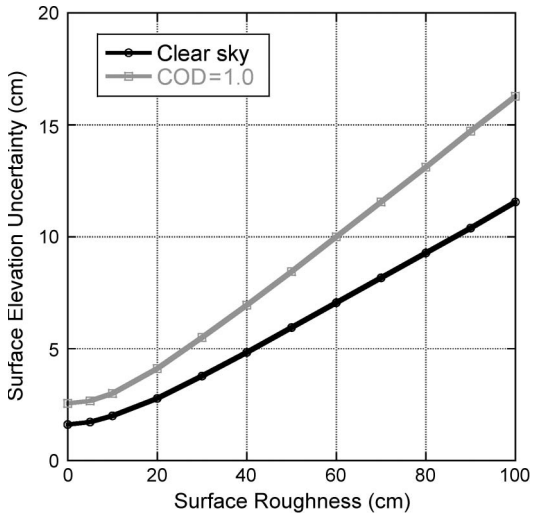

Fig. 12. Uncertainty of retrievals from 100 laser shot packets as a function of surface roughness. The black line is for clear sky, and the gray line is for cloudy sky with COD $= 1.0$. Cloud is at 0.5–1.0 km. The MODIS phase function with $r_e = 20$ μm was used.

need to be averaged so that the uncertainty can be lowered to a certain level, e. g., 2.0 cm? Fig. 13 shows the uncertainty as a function of averaging distance for surface roughness values of 10, 50, and 100 cm. As shown in Fig. 13(a), under clear-sky conditions, if the surface roughness does not exceed 10 cm, the uncertainty in the surface elevation retrieved with 100 laser shots is below 2.0 cm without further averaging. For the surface roughness values of 50 and 100 cm, however, to reach a 2.0-cm accuracy, the results need to be averaged over 0.63 and 2.38 km, respectively. Fig. 13(b) shows results for a cloudy-sky example with COD $= 1.0$. For this case, when the surface roughness is 10, 50, and 100 cm, in order to reach a 2.0-cm accuracy, the results need to be averaged over 0.21, 1.26, and 4.69 km, respectively.

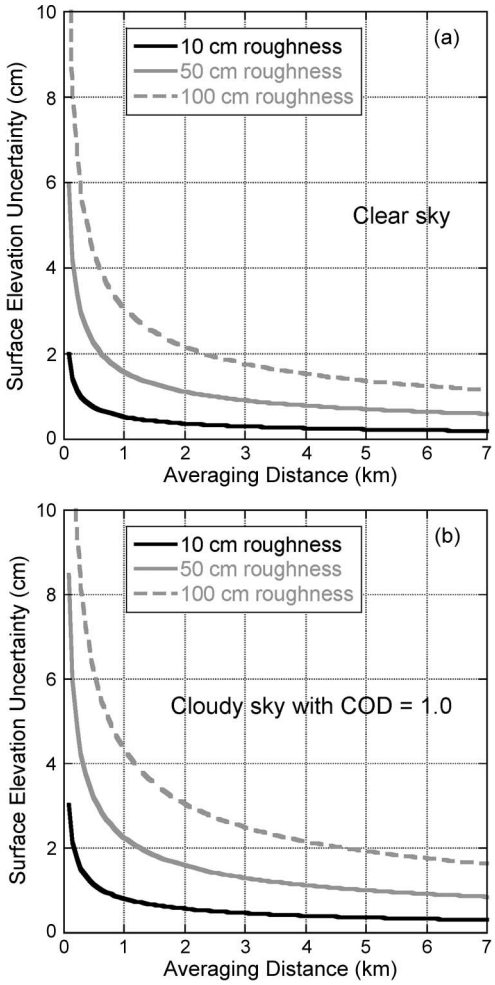

Fig. 13. Uncertainty of clear-sky surface elevation as a function of distance over which the retrievals are averaged for surface roughness of (solid black line) 10 cm, (solid gray line) 50 cm, and (dashed gray line) 100 cm. (a) For clear sky. (b) For cloudy sky with COD = 1.0. Cloud is at 0.5–1.0 km. The MODIS phase function with $r_e = 20$ μm was used.

We point out again that the simple surface roughness model used here does not represent the complexity of the real world. Rather, this model is used to help understand the basic impact of surface roughness on elevation retrieval when clouds are present. We are working on utilizing more advanced methods and field measurements [21]–[23] to further understand the problem.

The cloud detection process also brings uncertainties to the surface elevation retrievals [14]. A separation of clear and cloudy conditions is a fundamental step in the retrieval procedure. However, a perfect separation is essentially impossible [28], [29]. Any misclassification in the scene type will result in errors in the retrieved surface elevation [14]. We will report the research on ICESat-2 cloud screening separately. Aside from clouds, another weather phenomenon that has significant impact on surface elevation retrieval is blowing snow. Studies have shown that the effect of blowing snow could be much larger than clouds [14], [30]. The major difficulty in studying the effect of blowing snow is the lack of data over the ice sheets. However, the blowing snow detection method reported in [30] paves the way to an in-depth investigation on this topic.

VII. Summary

The current design of the ICESat-2 mission adopts a 532-nm micropulse photon-counting lidar with single photon capability for its surface elevation measurements. In support of the ICESat-2 mission, this paper establishes a framework that simulates the behavior of such a spaceborne lidar in cloudy and clear atmospheres. To investigate how clouds affect surface elevation retrieval, we first adopt the Poisson distribution for simulating the distribution of the number of arriving photons under clear-sky conditions. Second, our 3-D radiative transfer model is utilized in simulating the probability distribution of photon path length and the number of photon returns under cloudy-sky conditions. Third, the photon arrival time for each laser shot is determined with the Monte Carlo method, and surface elevation is derived through statistics of multiple laser shots. The main results of this study can be summarized as follows.

The ICESat-2 system's requirement of a photon probability of 0.8 for clear air over ice surface can be closely approximated by Poisson distribution with $\lambda = 1.5$.

Due to first photon bias, under clear sky, the retrieved surface elevation will appear higher. For simulations conducted in this study, the first photon bias for clear sky is $\sim$6.5 cm.

Clouds affect the surface elevation retrieved from the photon-counting system in two ways. First, clouds lower the average number of arriving photons. Having fewer arriving photons makes the surface appear lower compared with that for clear sky. Second, cloud forward scattering increases the photon path and makes the surface appear lower as well. The differences between clear- and cloudy-sky surface elevation retrievals are a function of cloud altitude and particle microphysics. For the simulations conducted here, the average surface elevation detected by the photon-counting system for cloudy sky with optical depth of 1.0 is 4.0–6.0 cm lower compared with that for clear sky.

If surface elevations are retrieved based on the statistics of 100 laser shots, the uncertainty is around 1.6 cm for clear sky; when clouds are present, the uncertainty increases. Both surface roughness and cloud detection process affect the uncertainty of the retrievals.

As a top priority NASA mission, ICESat-2 has a very high demand on system accuracy [31]. This study provides an understanding on the behavior of the photon-counting system in clear and cloudy atmospheres.

Acknowledgment

The authors would like to thank Dr. C. Chiu, Dr. M. McGill, and Dr. T. Martino for the helpful discussions and advice and Dr. U. Herzfeld and an anonymous reviewer for their comments.

References

[1] Goddard Space Flight Center, "Ice, cloud, and land elevation satellite," ICESat Brochure, 2002. [Online]. Available: http://icesat.gsfc.nasa.gov/icesat/education.php

[2] R. B. Alley, P. U. Clark, P. Huybrechts, and I. Joughin, "Ice-sheet and sea-level changes," *Science*, vol. 310, no. 5747, pp. 456–460, Oct. 2005. doi:10.1126/science.1114613.

[3] D. J. Quincey and A. Luckman, "Progress in satellite remote sensing of ice sheets," *Progr. Phys. Geography*, vol. 33, no. 4, pp. 547–567, Aug. 2009.

[4] H. J. Zwally, B. Schutz, W. Abdalati, J. Abshire, C. Bentley, A. Brenner, J. Bufton, J. Dezio, D. Hancock, D. Harding, T. Herring, B. Minster, K. Quinn, S. Palm, J. Spinhirne, and R. Thomas, "ICESat's laser measurements of polar ice, atmosphere, ocean, and land," *J. Geodyn.*, vol. 34, no. 3/4, pp. 405–445, Oct./Nov. 2002.

[5] B. E. Schutz, H. J. Zwally, C. A. Shuman, D. Hancock, and J. P. DiMarzio, "Overview of the ICESat mission," *Geophys. Res. Lett.*, vol. 32, p. L21 S01, 2005. doi:10.1029/2005GL024009.

[6] A. C. Brenner, J. P. DiMarzio, and H. J. Zwally, "Precision and accuracy of satellite radar and laser altimeter data over the continental ice sheets," *IEEE Trans. Geosci. Remote Sens.*, vol. 45, no. 2, pp. 321–331, Feb. 2007. doi:10.1109/TGRS.2006.887172.

[7] J. L. Bufton, J. E. Robinson, M. D. Femiano, and F. S. Flatow, "Satellite laser altimeter for measurement of ice sheet topography," *IEEE Trans. Geosci. Remote Sens.*, vol. GRS-20, no. 4, pp. 544–549, Oct. 1982. doi:10.1109/TGRS.1982.350423.

[8] D. C. Slobbe, R. C. Lindenbergh, and P. Ditmar, "Estimation of volume change rates of Greenland's ice sheet from ICESat data using overlapping footprints," *Remote Sens. Environ.*, vol. 112, no. 12, pp. 4204–4213, Dec. 2008. doi:10.1016/j.rse.2008.07.004.

[9] C. A. Shuman, H. J. Zwally, B. E. Schutz, A. C. Brenner, J. P. DiMarzio, V. P. Suchdeo, and H. A. Fricker, "ICESat Antarctic elevation data: Preliminary precision and accuracy assessment," *Geophys. Res. Lett.*, vol. 33, no. 7, pp. 10–13, 2006. doi:10.1029/2005GL025227.

[10] H. A. Fricker, T. Scambos, R. Bindschadler, and L. Padman, "An active subglacial water system in West Antarctica mapped from space," *Science*, vol. 315, no. 5818, pp. 1544–1548, Mar. 2007. doi:10.1126/science.1136897.

[11] Nat. Res. Council, *Earth Science and Applications From Space: National Imperatives for the Next Decade and Beyond*, 2007. prepared by the Committee on Earth Science and Applications from Space: A Community Assessment and Strategy for the Future, National Research Council, National Academies Press.

[12] D. P. Duda, J. D. Spinhirne, and E. W. Eloranta, "Atmospheric multiple scattering effects on GLAS altimetry—Part I: Calculations of single path bias," *IEEE Trans. Geosci. Remote Sens.*, vol. 39, no. 1, pp. 92–101, Jan. 2001.

[13] A. Mahesh, J. D. Spinhirne, D. P. Duda, and E. W. Eloranta, "Atmospheric multiple scattering effects on GLAS altimetry—Part II: Analysis of expected errors in Antarctic altitude measurements," *IEEE Trans. Geosci. Remote Sens.*, vol. 40, no. 11, pp. 2353–2362, Nov. 2002.

[14] Y. Yang, A. Marshak, T. Varnai, W. Wiscombe, and P. Yang, "Uncertainties in ice-sheet altimetry from a spaceborne 1064-nm single-channel lidar due to undetected thin clouds," *IEEE Trans. Geosci. Remote Sens.*, vol. 48, no. 1, pp. 250–259, Jan. 2010.

[15] L. Mandel, "Fluctuation of photon beams: The distribution of the photoelectrons," *Proc. Phys. Soc.*, vol. 74, no. 3, pp. 233–243, 1959.

[16] Z. Liu, W. Hunt, M. Vaughan, C. Hostetler, M. McGill, K. Powell, D. Winker, and Y. Hu, "Estimating random errors due to shot noise in backscatter lidar observations," *Appl. Opt.*, vol. 45, no. 18, pp. 4437–4447, Jun. 2006.

[17] C. P. Tsokos, *Probability Distributions: An Introduction to Probability Theory With Applications*. North Scituate, MA: Duxbury Press, 1972, pp. 111–119.

[18] R. F. Cahalan, L. Oreopoulos, A. Marshak, K. F. Evans, A. B. Davis, R. Pincus, K. H. Yetzer, B. Mayer, R. Davies, T. P. Ackerman, H. W. Barker, E. E. Clothiaux, R. G. Ellingson, M. J. Garay, E. Kassianov, S. Kinne, A. Macke, W. O'Hirok, P. T. Partain, S. M. Prigarin, A. N. Rublev, G. L. Stephens, F. Szczap, E. E. Takara, T. Várnai, G. Wen, and T. B. Zhuravleva, "The International Intercomparison of 3D Radiation Codes (I3RC): Bringing together the most advanced radiative transfer tools for cloudy atmospheres," *Bull. Amer. Meteorol. Soc.*, vol. 86, no. 9, pp. 1275–1293, Sep. 2005.

[19] Y. Yang, A. Marshak, J. C. Chiu, W. J. Wiscombe, S. P. Palm, A. B. Davis, D. A. Spangenberg, L. Nguyen, J. D. Spinhirne, and P. Minnis, "Retrievals of thick cloud optical depth from the Geoscience Laser Altimeter System (GLAS) by calibration of solar background signal," *J. Atmos. Sci.*, vol. 65, no. 65, pp. 3513–3527, Nov. 2008.

[20] B. A. Baum, P. Yang, A. J. Heymsfield, S. Platnick, M. D. King, Y. X. Hu, and S. T. Bedka, "Bulk scattering properties for the remote sensing of ice clouds. Part II: Narrowband models," *J. Appl. Meteorol.*, vol. 44, no. 12, pp. 1896–1911, Dec. 2005.

[21] U. C. Herzfeld, H. Mayer, W. Feller, and M. Mimler, "Glacier roughness surveys of Jakobshavns Isbrae drainage basin, West Greenland, and morphological characterization," *Zeitschrift für Gletscherkunde und Glazialgeologie*, vol. 35, no. 2, pp. 117–146, 1999.

[22] U. C. Herzfeld, H. Mayer, W. Feller, and M. Mimler, "Geostatistical analysis of glacier-roughness data," *Ann. Glac.*, vol. 30, no. 1, pp. 235–242, Jan. 2000.

[23] U. C. Herzfeld, "Master of the obscure—Automated geostatistical classification in presence of complex geophysical processes," *Math. Geosci.*, vol. 40, no. 5, pp. 587–618, 2008. doi:10.1007/s11004-008-9174-4.

[24] B. A. Campbell, "Scale-dependent surface roughness behavior and its impact on empirical models for radar backscatter," *IEEE Trans. Geosci. Remote Sens.*, vol. 47, no. 10, pp. 3480–3488, Oct. 2009. doi:10.1109/TGRS.2009.2022752.

[25] M. B. Rivas, J. A. Maslanik, J. G. Sonntag, and P. Axelrad, "Sea ice roughness from airborne LIDAR profiles," *IEEE Trans. Geosci. Remote Sens.*, vol. 44, no. 11, pp. 3032–3037, Nov. 2006. doi:10.1109/TGRS.2006.875775.

[26] C. J. van der Veen, Y. Ahn, B. M. Csatho, E. Mosley-Thompson, and W. B. Krabill, "Surface roughness over the northern half of the Greenland Ice Sheet from airborne laser altimetry," *J. Geophys. Res.*, vol. 114, no. F1, p. F01 001, 2009. doi:10.1029/2008JF001067.

[27] D. Yi, H. J. Zwally, and X. Sun, "ICESat measurement of Greenland Ice Sheet surface slope and roughness," *Ann. Glac.*, vol. 42, no. 1, pp. 83–89, Aug. 2005.

[28] Y. Yang, L. Di Girolamo, and D. Mazzoni, "Selection of the automated thresholding algorithm for the multi-angle imaging spectroradiometer radiometric camera-by-camera cloud mask over land," *Remote Sens. Environ.*, vol. 107, no. 1/2, pp. 159–171, 2007.

[29] Y. Yang and L. Di Girolamo, "Impacts of 3-D radiative effects on satellite cloud detection and their consequences on cloud fraction and aerosol optical depth retrievals," *J. Geophys. Res.*, vol. 113, p. D04 213, 2008. doi:10.1029/2007JD009095.

[30] S. P. Palm, Y. Yang, J. Spinhirne, and A. Marshak, "Satellite remote sensing of blowing snow properties over Antarctica," *J. Geophys. Res*, in press.

[31] W. Abdalati, H. J. Zwally, R. Bindschadler, B. Csatho, S. L. Farrell, H. A. Fricker, D. Harding, R. Kwok, M. Lefsky, T. Markus, A. Marshak, T. Neumann, S. Palm, B. Schutz, B. Smith, J. Spinhirne, and C. Webb, "The ICESat-2 laser altimetry mission," *Proc. IEEE*, vol. 98, no. 5, pp. 735–751, May 2010. doi:10.1109/JPROC.2009.2034765.

Yuekui Yang received the B.S. and M.S. degrees in atmospheric sciences from the Science and Engineering University of the Army, Nanjing, China, in 1987 and 1990, respectively, and the Ph.D. degree in atmospheric sciences from the University of Illinois at Urbana–Champaign, Urbana, in 2007.

He was a Research Scientist with the Aviation Meteorological Research Institute, Beijing, China, from 1990 to 1997, a Software Engineer with the Beijing METSTAR Radar Company, Ltd., from 1997 to 1999, and a Project Manager with Datatrust Information Technologies, Beijing, from 1999 to 2001. He has been with the NASA Goddard Space Flight Center, Greenbelt, MD, since 2007, first as a faculty member of the Goddard Earth Sciences and Technology Center, University of Maryland, Baltimore County, and now as an Assistant Research Scientist with the Universities Space Research Association, Columbia, MD. His research experience includes radiative transfer modeling, satellite cloud detection, and study on polar clouds and blowing snow with both passive and active remote sensing instruments.

Alexander Marshak received the M.S. degree in applied mathematics from the University of Tartu, Tartu, Estonia, in 1978 and the Ph.D. degree in numerical analysis from the Soviet Academy of Sciences, Novosibirsk, Russia, in 1983.

In 1978, he joined the Institute of Astrophysics and Atmospheric Physics, Estonia, and worked there for 11 years. In 1989, he received an Alexander von Humboldt fellowship and worked for two years with the University of Göttingen, Göttingen, Germany. He joined the NASA Goddard Space Flight Center (GSFC), Greenbelt, MD, in 1991, first working for the Science Systems and Applications, Inc., then the Joint Center for Earth Systems Technology, University of Maryland, Baltimore County, and finally, NASA GSFC where he has been employed since 2003. He has published over 100 refereed papers, books, and chapters in edited volumes.

Stephen P. Palm received the B.S. degree in physical science and M.S. degree in meteorology from the University of Maryland, Baltimore, in 1979 and 1985, respectively.

He has been with the NASA Goddard Space Flight Center, Greenbelt, MD, since 1979 and has worked primarily on lidar remote sensing of atmospheric clouds, aerosols, and boundary layer dynamics. He is also with Science Systems and Applications, Inc., Lanham, MD. He was a member of the ICESat and CALIPSO Science Teams and is currently a member of the ICESat-2 Science Definition Team. He was the Leader of the Geoscience Laser Altimeter System (GLAS) atmospheric algorithm group and the main developer of the software for the near-real-time production of level 1 and 2 GLAS atmospheric data products. He also is the Lead Author of the GLAS Algorithm Theoretical Basis Document and the GLAS Atmospheric Data Products Validation Plan. His main interests include polar climate, cloud–sea ice interaction, and blowing snow detection using satellite remote sensing.

Tamás Várnai received the M.S. degree equivalent diploma in meteorology from Eötvös Loránd University, Budapest, Hungary, in 1989, and the Ph.D. degree in atmospheric and oceanic sciences from McGill University, Montreal, Canada, in 1996.

From 1989 to 1991, he was a Research Scientist with the Hungarian Meteorological Service. From 1997 to 1999, he was a Postdoctoral Fellow with The University of Arizona, Tucson. In 1999, he moved to the Joint Center for Earth System Technology of the University of Maryland, Baltimore County, and of the NASA Goddard Space Flight Center, Greenbelt, MD, where he is currently a Research Associate Professor of Physics. His research interests focus on 3-D radiative processes in clouds and on remote sensing of cloud properties.

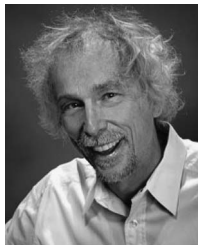

Warren J. Wiscombe received the B.S. degree in physics from the Massachusetts Institute of Technology, Cambridge, in 1964, and the M.S. degree in physics and the Ph.D. degree in applied mathematics from the California Institute of Technology, Pasadena, in 1966 and 1970, respectively.

From 1969 to 1975, he was a Research Scientist with Systems, Science and Software, La Jolla, CA. He was a Staff Scientist with the National Center for Atmospheric Research from 1974 to 1980. He was then an Associate Professor with the Department of Applied Sciences, New York University, New York, from 1980 to 1984. In 1984, he joined the NASA Goddard Space Flight Center, Greenbelt, MD, as a Senior Research Scientist. His research covers radiative transfer, light scattering, cloud radiation, climate theory, remote sensing, and science data systems.

Dr. Wiscombe has been a fellow of the American Meteorological Society since 1989.